World Academy of Science, Engineering and Technology
International Journal of Biomedical and Biological Engineering
Vol:6, No:11, 2012

Contrast-Enhanced Multispectal Upconversion Fluorescence Analysis for High-Resolution In-Vivo Deep Tissue Imaging

Lijiang Wang, Wei Wang, and Yuhong Xu

***Abstract*—**Lanthanide-doped upconversion nanoparticles which can convert near-infrared lights to visible lights have attracted growing interest because of their great potentials in fluorescence imaging. Upconversion fluorescence imaging technique with excitation in the near-infrared (NIR) region has been used for imaging of biological cells and tissues. However, improving the detection sensitivity and decreasing the absorption and scattering in biological tissues are as yet unresolved problems. In this present study, a novel NIR-reflected multispectral imaging system was developed for upconversion fluorescent imaging in small animals. Based on this system, we have obtained the high contrast images without the autofluorescence when biocompatible UCPs were injected near the body surface or deeply into the tissue. Furthermore, we have extracted respective spectra of the upconversion fluorescence and relatively quantify the fluorescence intensity with the multispectral analysis. To our knowledge, this is the first time to analyze and quantify the upconversion fluorescence in the small animal imaging.

***Keywords*—**Multispectral imaging, near-infrared, upconversion fluorescence imaging, upconversion nanoparticles.

I. Introduction

FLUORESCENCE imaging has provided a facile method for visualizing complex biological processes at the molecular level, so it is a very important technique for biological studies and clinical applications due to its high temporal and spatial resolution [1]-[2]. Conventional fluorescence imaging is based on single-photon excitation, emitting low energy fluorescence when excited by a high energy light, and the classic fluorescent labels include various organic dyes[3], metal complexes [4], and semiconductor quantum dots (QDs, such as CdS, CdSe, CdTe)[5]-[6]. However, these also have some intrinsic limitations, for example, tissue damage caused by long-term irradiation of UV or short wavelength light, significant auto-fluorescence background to mask the signals from the fluorescent probes, and short penetration depth of short wavelength excitation light in biological tissues. As to luminescent labels, the main drawback of organic dyes is photobleaching, while QDs are still controversial due to their inherent toxicity and chemical instability. The recent superior strategy is to develop two-photon fluorescence imaging which converts low energy light, usually NIR, into higher-energy light (visible) through sequential absorption and energytransfer steps [7]. NIR radiation is less harmful to biological specimen, minimizes background autofluorescence and penetrates tissues or animal bodies to a greater extent [8].

Upconversion nanoparticles(UCPs) are luminescent nanomaterials which convert a NIR excitation into a visible emission through lanthanide doping [9]. Such a unique luminescent mechanism excludes both conversional luminescent labels and endogenous fluorescent substances. Recently, UCNPs have been proposed as a new generation of biological luminescent labels and used for bioimaging in living cell or in vivo[10]-[12], due to their attractive chemical and optical features, such as low toxicity, sharp absorption and emission lines, long lifetimes, and superior photostability. For upconversion fluorescence imaging, UCPs should meet two main requirements: (I) good dispersibility in aqueous solutions, and (II) the presence of some functional groups (such as–COOH, $–NH_2$, or –SH) on their surface to allow further conjugation with biologically active molecules. The advancement in the nanoparticles synthesis has been very encouraging, and with the gradual perfection of techniques about surface modification, UCPs have been improved to own better dispersibility inwater and more harmonious surface properties for functionalization and bioconjugation. Safety issues related to the nanomaterials application are always being highlighted and concerned, recent some cytotoxicity and biodistribution studies have demonstrated UCPs have good biocompatibility in vitro and in vivo bioimaging. The ubiquitous autofluorescence signals that degrades performance in conventional fluorescence-based small-animal imaging systems can primarily be attributed to components of the skin (mostly collagen), as well as to food (mostly chlorophyll-breakdown-products) and to porphyrins, which will obey Stokes' law. So far, there is no protein or other molecular with upconverting characteristic to be found in the biological tissue. In theory, no or less background fluorescence will be produced when the biological sample is excited by the NIR light. The "optical transmission window" of the biological tissues falls within the NIR range (λ =750～1000nm), which allows for deeper light penetration, lower autoflurescence and

Lijiang Wang is with the Zhejiang California International Nanosystems Institute, Zhejiang University, Hangzhou 310027, PR China (e-mail: wdwtms @zju.edu.cn).

Wei Wang is with the Zhejiang California International Nanosystems Institute, Zhejiang University, Hangzhou 310027, PR China (e-mail: zcni.wangwei@gmail.com).

Yuhong Xu is with the Zhejiang California International Nanosystems Institute, Zhejiang University, Hangzhou 310027, and also with the *School of Pharmacy, Shanghai Jiao Tong University, Shanghai 200240,* PR China(phone:+86-571-86971897;fax: +86-571-86971897; e-mail: iyuhongxu@gmail.com).

photodamage, reduced light scatterering, and increased image contrast. Autofluorescence is one of the most important factors influencing the imaging sensitivity, while this problem is not existed in the upconversion imaging because the UCPs are excited by the 980nm NIR laser. Consequently, it is reasoned that UCPs constitute one of the most promising classes of fluorescence biomaterials applied in biological labelling and imaging. However, in the process of upconversion fluorescence imaging, challenges still remain in obtaining high contrast optical imaging with quantitative analysis and decreasing light scattering. At the same time, another hurdle is the absence of widespread commercial readers for assay analysis. UV excitation and visible emission detection are used in most fluorescence-based assays, which are not suitable for upconverting materials.

The multispectral imaging (MSI) technique, which delivers a high-resolution optical spectrum at every pixel of an image, can remove the signal degradation caused by autofluorescence while adding enhanced multiplexing capabilities. It is an approach that optimizes the opportunities for multiplexing while at the same time overcoming the effects of autofluorescence on detectability and reliable quantitation. A series of images of a particular field can be rapidly acquired at different wavelengths to create a spectral date "cube", in which the 3 dimensions are x, y and wavelength. In this cube, a spectrum is associated with every pixel. The resulting data can be used to identify, separate and remove the contribution of autofluorescence in analyzed images. In addition, simple image analysis tools applied to each channel can be used to extract all relevant measures from regions of interest such as intensity (maximum, average, total), area, dimension, etc. Based on multispectral imaging technique, Cambridge Research&Instrumentation, Inc. (CRi) has manufactured the Maestro™ *in vivo* imaging system for small animal imaging, which is very beneficial to promote the molecular-based drug and diagnostic research. Whereas, the wavelength range of excitation light is from 450 to 850nm, so at present the Maestro™ system is inapplicable for the *in vivo* imaging with upconversion fluorescence labels. In the present study, we attended to explore the improvement and use of the MSI technique for in vivo upconversion fluorescence imaging, and try to obtain the high contrast optical imaging with the lack of background autofluorescence. Furthermore, we can extract respective spectra of the upconversion fluorescence and relatively quantify the fluorescence intensity with the multispectral analysis. To our knowledge, this is the first time to analyze and quantify the upconversion fluorescence in the small animal imaging.

II. Materials and Methods

A. Chemicals and Reagents

Trioctylphosphine oxide (TOPO) (90%) and trifluoroacetic acid (CF_3COOH, reagent grade) were purchased from Sigma-Aldrich. 99.99% Ln_2O_3 (Ln = Tm^{3+},Er^{3+},Ho^{3+}) were provided by Aladdin reagent company. Tetraethyl orthosilicate (TEOS) were ordered from Alfa Aesar. Other reagents were all from Sangon. All the reagents were used as received without further purification. CF_3COOLn precursors were prepared by dissolving the corresponding lanthanide oxides in trifluoroacetic acid and heating at the reflux temperature. After clear solutions were obtained, the solvent was removed under vacuum. The resulting solids were dried under vacuum at room temperature overnight and used without further purification.

B. Animal

All in vivo experiments were performed in compliance with Zhejiang University Animal Study Committee's requirements for the care and use of laboratory animals in research. Eight to twelve weeks old athymic nude mice (Balb/c, shanghai Slac laboratory animal center) weighing from 15 to 25 g were used in these experiments. Mice were kept in 12 h light/dark cycle and had access to food and water ad libitum before the experimentation. Three groups of animals, each composed of five mice, were used for in vivo imaging study: one control group who received only phosphate buffer saline (PBS), and two experimental groups injected with UCPs. All experiments were performed under anesthetic using intraperitoneal injection with the solution containing 2% Pelltobarbitalum Natricum (45mg/kg of body weight).

C. Development of the NIR-reflected Multispectral Imaging System

In vivo upconversion fluorescence imaging was performed with a modified NIR-reflected multispectral imaging system designed by our group. Fig. 1 shows the diagram of this equipment, which mainly includes three portions: the excitation source, the filter and reflecting set and the Maestro multispectral imaging system (CRi Inc.). One external 0-2000 mW adjustable 980 nm optical fiber-coupled laser (Changchun Mingwan Optics Co., China) were used as the excitation source and the beam was focused to a spot size of approximately 5 cm. The filter and reflecting set is consisted of some bandpass emission filters, which has a heat coating to prevent the interference of excitation light to the CCD camera. Images of fluorescence signals are recorded using cold CCD and analyzed by Maestro multispectral imaging system. Animal-to-laser distance was fixed using a ruler attached to the laser head.

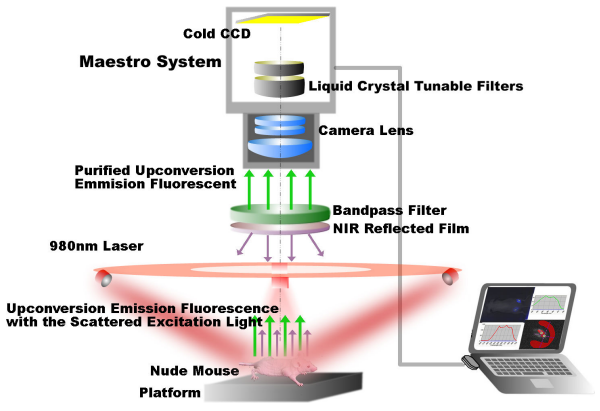

Fig. 1 The diagram of NIR-reflected Multispectral Imaging System

D. Synthesis of NaYF4: Yb, Ln (Ln = Tm3, Er3+, Ho3) UCPs

A mixture of 1.25 mmol CF3COONa, 0.48 mmol (CF3COO)3Y, 0.12 mmol (CF3COO)3Yb, and 0.00024 mmol (CF3COO)3 Ln (Ln = Tm3+,Er3+,Ho3+)) was dissolved in 10g TOPO. Under vigorous stirring in a 50 ml flask, the mixture was first heated at 100℃under vacuum for 30 min to remove water, and then argon was purged into the solution periodically. In the presence of argon, the solution was then heated to the targeted temperature (360℃) within 30 min. All the reactions were stopped after one hour of heating at the desired temperature. Chloroform and Methanol were added to dissolve the reaction product and precipitate the nanoparticles, respectively. The nanoparticles were isolated by centrifugation and were washed with ethanol at least three times.

E. Surface Modification of NaYF4: Yb, Ln (Ln = Tm3+, Er3 ,Ho3+) UCPs

The synthesized NaYF4: Yb, Ln (Ln =Tm3+,Er3+,Ho3+) upconversion nanoparticles should be primarily modified with active groups, such as amine (-NH2) and carboxyl (-COOH) groups to become water-soluble and biocompatible .

A water-in-oil microemulsion was prepared by mixing 1ml Co-520, 1.8ml cyclohexane and 4ml 0.01M UCPs solution in 7.5ml cyclohexane and stirring for 10min. Then 0.5ml Co-520 and 0.08ml ammonia were added and sonicated to form a transparent emmusion. After adding 40ul TEOS into the solution, this reaction was allowed to continue for 48h at room temperature (RT) with stirring. Finally, the reaction mixture was added with acetone at 1:1 volume ratio and centrifuged at 10000rpm for 30min. The pellet was washed by ethanol/ DI water solution (1:1) at least three times and dispersed into the DI water. Thus the hydrophobic UCPs were converted into hydrophilic ones.

F. Characterization

Transmission electron microscopy (TEM) images were recorded on a JEOL/JEM-1230 transmission electron microscope. High-resolution TEM (HRTEM) and Energy Disperse Spectroscopy (EDS) were carried out using a JEOL/JEM-2010F TEM operating at an acceleration voltage of 200 kv. X-ray powder diffraction (XRD) was performed for crystal phase identification by THEMO ELECTRON/ ARL X'TRA x-ray powder diffractometer. Upconversion fluorescence spectra were obtained using a Hitachi F-4600 fluorescence spectrophotometer equipped with an external 980 nm laser as the excitation source.

G. Small Animal Imaging and Multispectral Analysis

For upconversion fluorescence imaging near the body surface, athymic nude mice were anaesthetized and injected subcutaneously with 100μl aqueous solution of UCPs (4.4 mg ml-1) at the regions of upper legs. To confirm the feasibility of deep-tissue imaging, 100μl aqueous solution of UCPs were injected into the pleural cavity of the mude mice. The depth of injection was about 1cm estimated from needle penetration. Upconversion luminescence was observed in a darkened room, and recorded using the NIR-reflected multispectral imaging system. The laser power density was ~0.2 W/cm^2 during imaging, which was a safe power to protect the animal body. In vivo spectral imaging from 450 to 850 nm (10 nm step) was carried out with an exposure time of 1000 ms for each image frame. Note that the exposure time required for upconversion imaging is generally much longer than that required for other fluorescence imaging, due to the rather low quantum yield of UCPs. Multicolor images were obtained by introducing spectra of individual UCP complexes for spectra unmixing using the software attached to the multispectral imaging system. At the end of the experiments, the animals were euthanized according to standard approved protocol.

III. Results and Discussion

A. Synthesis and Characterization of UCPs

For biological applications, the desired upconverting nanoparticles should have a suitable size and feasibleble surface for conjugation with biological molecules, and exhibit highintensity emission as well. The first step to synthesize UCPs is the selection of an efficient host for lanthanide ions. Recent reports have expatiated that the colloidal $NaYF_4$ nanoparticle hosts in either the α-phase or the β-phase doped with Yb, Ln (Ln = Er^{3+}, Ho^{3+}, and Tm^{3+}) are so far the best candidates for biological applications. Furthermore, the β-phase nanoparticles present higher upconverting efficiency than those of the α-phase due to the more symmetric β-phase structure. In order to obtain small and β-phase NaYF4: Yb, Ln (Ln = Tm) UCPs, we have adopted the co-thermolysis method using the solvent of TOPO because it has higher boiling temperature (200℃/2 mm Hg) and coordination properties for the selective synthesis of β-phase nanoparticles. The role of TOPO was to provide surface binding and spatial restriction on the nanoparticles to ensure monodispersed growth of the β-phase nanoparticles. TEM image of the synthesized UCPs is shown in Fig.2A. It can be seen that the nanoparticles prepared in TOPO are highly monodisperse with the average size of about 10nm. The HRTEM image in Fig.2B shows the crystalline fringes of the UCPs, which demonstrate legible crystal lattice of the nanoparticles produced in TOPO solvent. The UCPs synthesized in TOPO solvent is smaller than those by other approaches, thus they are more suitable for biological applications.

Taking $NaYF_4$:Yb,Tm nanoparticles for example, the EDS pattern for this sample confirms that the nanoparticles are composed exclusively of Na, Y, Yb, F and Tm (Fig. 2C). The crystalline structures of the $NaYF_4$:Yb,Tm nanoparticles were determined using x-ray diffraction (XRD), and the pattern given in Fig. 2D has suggested a high crystallinity of the nanoparticles. A hexagonal NaYF4 phase is considered to be the dominant phase without the presence of the cubic phase. Fig. 3 gives the upconversion fluorescence spectra and photograph of the $NaYF_4$:Yb, Ln (Ln =Tm^{3+}, Ho^{3+}, Er^{3+}) solutions excited with a 980 nm NIR laser, showing the strong visible colorful fluorescence from the nanoparticles. Based on above-mentioned results, we could conclude that the TOPO, as the solvent and ligand, controlled the selective crystalline growth and provided the flexibility for the synthesis of β-phase nanoparticles, which led to much more efficient formation of

UCPs in small particle size (~10nm) and with a narrow size distribution.

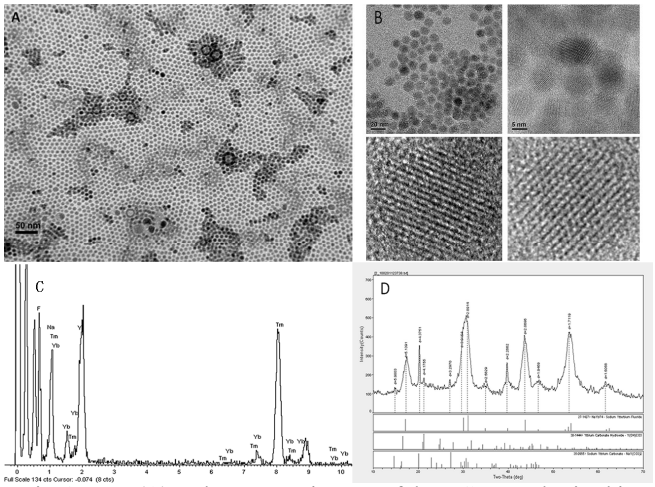

Fig. 2 TEM (A) and HR-TEM images of the UCPs synthesized in TOPO solvent. EDS(C) and XRD(D) patterns of $NaYF_4$:Yb,Tm sample synthesized in TOPO solvent

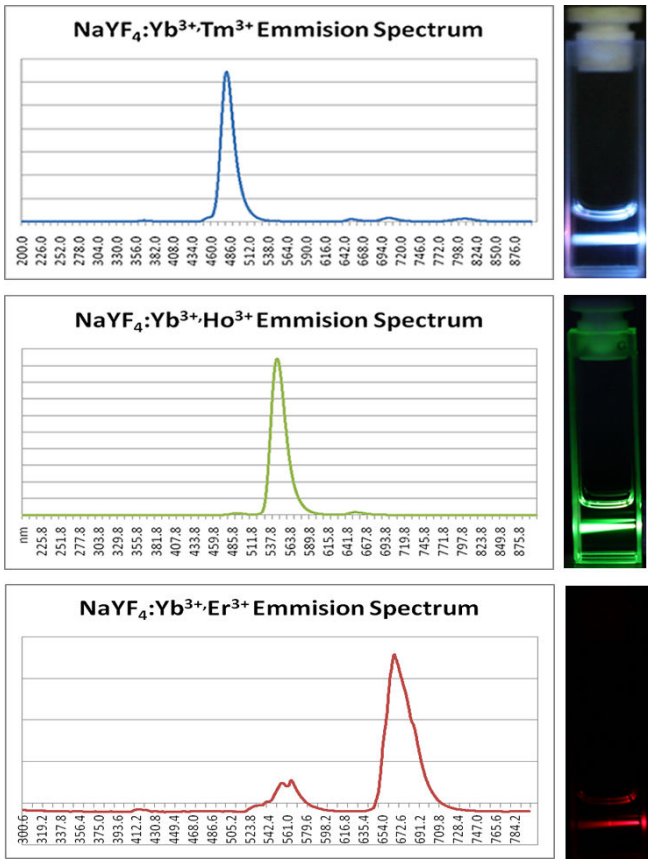

Fig. 3 Fluorescence spectra and photograph of the UCPs when excited by a NIR laser at 980 nm

B. Surface Modification of UCPs

In order to have biological applications, the nanoparticles must be water-soluble, biocompatible and photostable. The synthesized UCPs we have obtained by the co-thermolysis method in TOPO solvent are hydrophobic in solutions. It is therefore necessary to modify the surfaces of these nanoparticles with active functional groups or ligands. The surface properties determine the solubility of the nanoparticles in physiologic solutions, stability over time and different pH conditions, and the ability to provide anchors for adding functional ligands such as antibodies and drugs. For surface modification, SiO_2 shells are generally grown on the surfaces of nanoparticles by cohydrolysis and polycondensation with TEOS, and then the linkage groups pointing outwards are adhered to the surfaces of the SiO_2 shells. Thus, the modified nanoparticles can be more readily conjugated with biomolecules and used as highly fluorescent, sensitive, and reproducible biolabels. From the TEM micrograph in Fig.4, it can be seen that these well-dispersed spherical nanoparticles are coated by a uniform SiO_2 shell layer with a mean diameter of about 50 nm, and have formed a clear, aggregate free solution in water. This result has showed that these are well-dispersed spherical nanoparticles with a mean diameter of about 30 nm after surface modification. It was worth to be mentioned that surface modification can provide the nanoparticles with high solubility in solutions and never decrease upconversion fluorescence in our experiments. When excited with a 980nm NIR laser, the nanoparticles have emitted strong upconversion fluorescence at 550nm (green) and 650nm (red), and the whole solutions are very clear and transparent. These nanoparticles have been chosen for subsequent experiments.

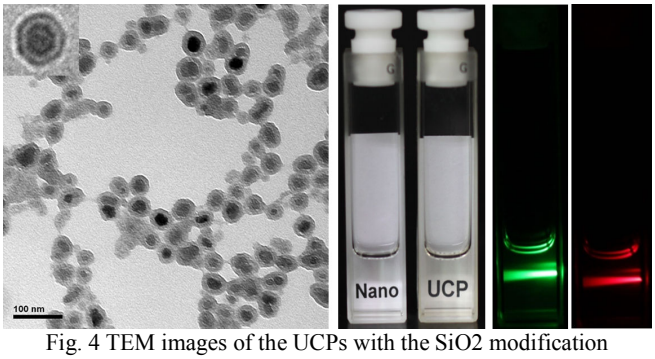

Fig. 4 TEM images of the UCPs with the SiO2 modification

C. Animal Imaging and Multispectral Analysis

Our ultimate goal is to perform fluorescent imaging of small animals. To demonstrate the suitability and effectiveness of using the UCPs for in vivo imaging, anaesthetized nude mice were injected subcutaneously at the upper leg regions with 100 µl aqueous solution of NaYF4: Yb, Er nanoparticles (4.5 mg ml-1) in the left and the same amount of $NaYF_4$: Yb, Ho nanoparticles in the right. The depth of injection was estimated from needle penetration and all data were collected using the NIR-reflected Multispectral Imaging System. We have adopted one special bandpass filter with the infrared reflected coating film. This bandpass filter is designed to selectively transmit a specific range of wavelengths spanning the peak emission of the UCPs, and block light on either side of that range. In upcoversion imaging, the UCPs are excited by a 980nm NIR laser. If the power of light source is too high, more scattering excitation light will transmit the filter and reach the highsensitive CCD. Actually, the CCD itself is not selective for the spectrum, and the emission intensity may be far lower than that of the proportion of the excitation light through the filter. As a result, the distortion of UCP imaging

will turn up. In other words, the CCD has just captured the false emission light. To solve this problem, a layer of optical film to reflect the 980 infrared light has been coated onto the filter surface. In terms of theory, this coating has the unique ability to reflect the scattering light from the excitation point, but transmit the emitted fluorescence. Even if partial excitation light has transmitted the film, it will be removed by the emission filter, which greatly enhances the detection sensitivity to UCP emission spectra.

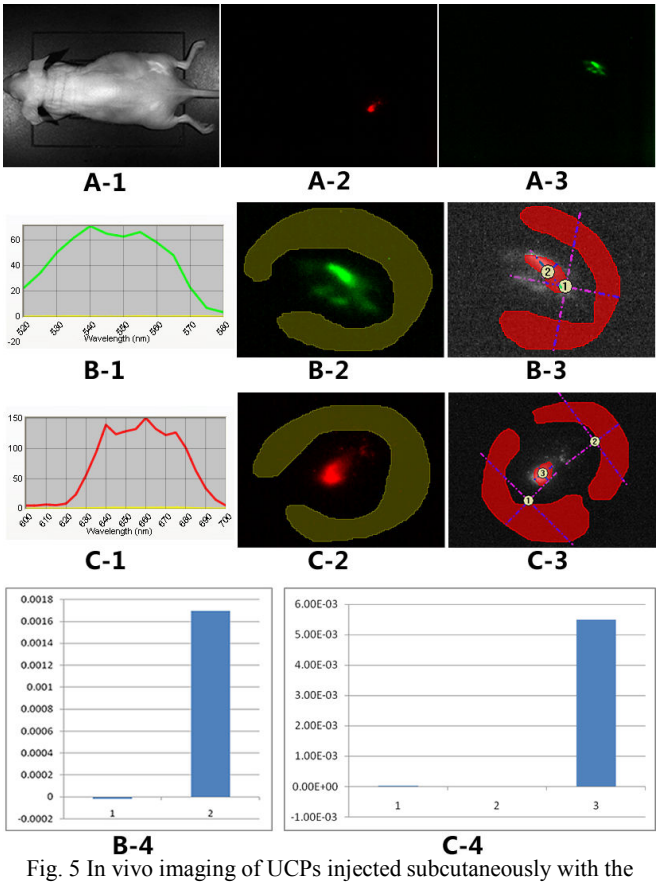

Fig. 5 In vivo imaging of UCPs injected subcutaneously with the multispectral analysis (A-1: the white image; A-2, A-3: red and green visible fluorescence by scanning the corresponding waveband of emission light; B-1, C-1: the "purified" spectra of NaYF4: Yb, Ho nanoparticles (green), NaYF4: Yb, Er nanoparticles (red); B-2, C-2: the area within the yellow circle is the region without luminescence; B-3, C-3: labeling the fluorescence regions and the environmental area without luminescence; B-4, C-4: S/N values of green and red fluorescence.)

A representative nude mouse at white light is shown in Fig. 5A-1, and nanoparticles injected subcutaneously into upper legs of the mouse have showed red and green visible fluorescence by means of separately scanning the corresponding waveband of emission light (Fig. 5A-2,3). Spectral unmixing, which is an important function of Maestro spectral imaging system, can take signals that may overlap both spatially and spectrally, and separate them faithfully, without crosstalk. It is achievable to obtain accurate spectra for each fluorescence signal in the image using the compute-pure-spectra (CPS) tool. As showed in Fig. 5B-2 and C-2, the area of green fluorescence is the signal region arising from

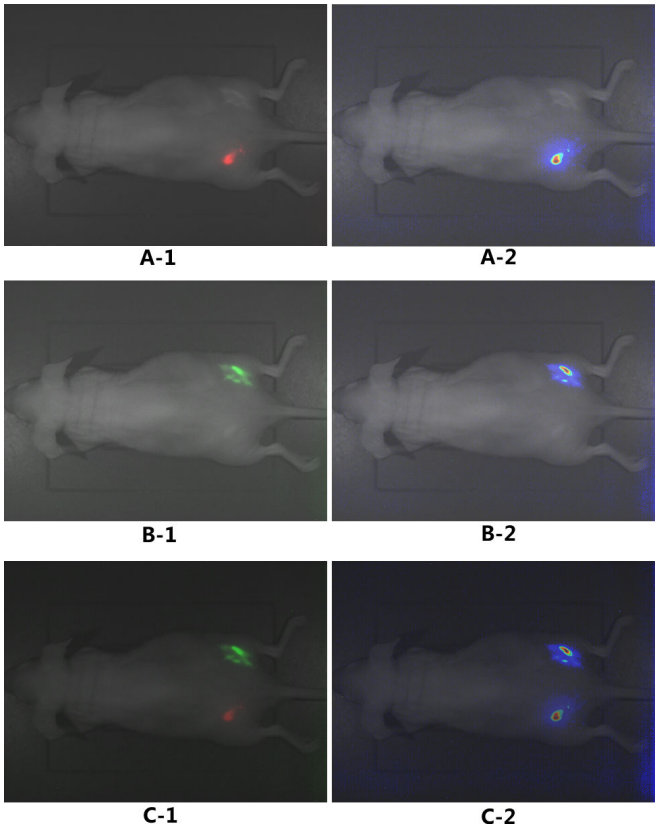

Fig .6 The composite images formed from the upconversion images and the white light image (A-1, B-1, C-1). The composite images formed from the intensity distribution images and the white light image (A-2, B-2, C-2)

$NaYF_4$: Yb, Ho nanoparticles, while the red area is from $NaYF_4$: Yb, Er nanoparticles. These images were acquired by the Maestro imaging system after spectral unmixing. The delimited area within the yellow circle around the fluorescence signal region is the segment without luminescence when it is exposed to the 980nm NIR laser. The Fig5B-1 and C-1 show the "purified" spectra of $NaYF_4$: Yb, Ho nanoparticles (green), $NaYF_4$: Yb, Er nanoparticles (red). These spectra are consistent with the preceding emission spectra of UCPs, which indicate that these fluorescence signals are certainly caused by the upconversion emission. Extracting the spectra dissection data of the peak emission wavelength (550nm and 650nm), and labeling the fluorescence regions and the environmental area without luminescence respectively (Fig. 5B-3, C-3), then the average counts signals can be obtained by detection of the fluorescence signal intensity. As revealed from the maps of the measured fluorescence signal intensity with the corresponding area, the signal-to-noise ratio (S/N) of green fluorescence area is 107(Fig. 5B-4), while the S/N value of red fluorescence runs up to 1346(Fig. 5C-4). These data clearly show that the background fluorescence intensity is very close to the system fluctuation noise. So in our upconversion imaging, there is almost no autofluorescence signal outside the interesting area, and an excellent fluorescence signal can be acquired when the UCPs are injected subcutaneously in the live small animal. Even in the range very close to the target fluorescence region, high S/N values could still be obtained. These weak noises are

probably produced by the feeble scattered light of target fluorescence or the interference of excitation light through the filter. Because of the absence of autofluorescence, the morphology of nude mice is invisible in upconversion fluorescence images (Fig 5A-2 and A-3). The composite images formed from the upconversion images and the white light image shows the locations of UCPs fluorescence signals clearly (Fig. 6A-1, B-1, C-1), meanwhile the intensity distribution features of the upconversion fluorescence can be investigated from the corresponding intensity pattern(Fig. 6A-2, B-2, C-2).

The fluorescence signals arising from the UCPs injected subcutaneously could be captured by our NIR-reflected multispectral imaging system, and the spectra and intensity data of regions interested were obtained by means of spectral analysis. As a model, some valuable characteristic of the upconversion imaging in small-animal have been validated successfully, such as the absence of autofluorescence and the high signal-to-noise ratio. Owing to these advantages in vivo imaging, UCPs are particularly well suited for background-free signal collection while at the same time allowing us to image deeper into tissue. 100μl aqueous solution of NaYF4: Yb, Ho nanoparticles and 100μl NaYF4: Yb, Er nanoparticles were injected into the pleural cavity of two different nude mice. As shown in Fig.7A-2 and Fig.8A-2, the green and red fluorescence image is originated from the UCPs after spectral unmixing. Tagging the fluorescence area and the environmental background regions (Fig.7C-1 and Fig.8C-1), and measuring the fluorescence signal intensity separately, then the average counts signal could be obtained. The S/N value of green fluorescence arising from the NaYF4: Yb, Ho nanoparticles injected into the deep tissue is 18.5(Fig.7C-2), which is lower than that of ones injected subcutaneously. The reasons for the decline of imaging sensitivity may be the absorbing and scattering properties of tissue, and the limited penetrating ability of emission light (550nm). The S/N value of red fluorescence arising from the NaYF4: Yb, Er nanoparticles is 96.5(Fig.8C-2), which is much higher than that of green fluorescence. The significant S/N improvement allows NaYF4: Yb, Er nanoparticles more appropriate for deep-tissue imaging. There are some important factors determining such result: 1) the UCPs with red emission light have a high quantum yield, thus the higher fluorescence intensity could be obtained; 2) the tissue penetrability of red emission light has been enhanced as the emission wavelength is increased (650nm), so it is easier to be captured by the CCD. At the same time, high signal to noise ratio could be obtained with the lack of auto fluorescence, thereby the nanoparticles with red emission light have the favorable potential to be used in deep-tissue imaging. As shown in Fig 7B-1, B-2 and Fig 8B-1, B-2, the white images were merged with the upconversion fluorescence and intensity distribution images.

We have showed the feasibility of using biocompatible upconverting nanoparticles for mice imaging with our NIR-reflected multispectral imaging system, and obtained the high contrast results without the autofluorescence. Much can be done to improve the animal experiments: to continuously image subcutaneous and muscular tissues in real time; to innovate safer and specific probes for tumor imaging and treatment; to synthesize smaller UCPs with high luminescence intensity; to explore more popular and effective methods for the surface modification of UCPs with less energy loss; to develop a mobile imaging platform to record the scans of small-animals, etc. Continuous live imaging of tissues in small animal models can be utilized in monitoring of tumors and exploration of pathologies without unnecessary sacrifice of animals—particularly important where temporal series of data are necessary. Scale and brightness are the important hurdles in the bioapplication of UCPs, so the research of synthesis and surface modification will help to promote the development of UCPs for in vitro and in vivo use. With growing use and popularity of UCPs, it is hoped that more standard and versatile equipment will emerge and help in the development of this promising technology.

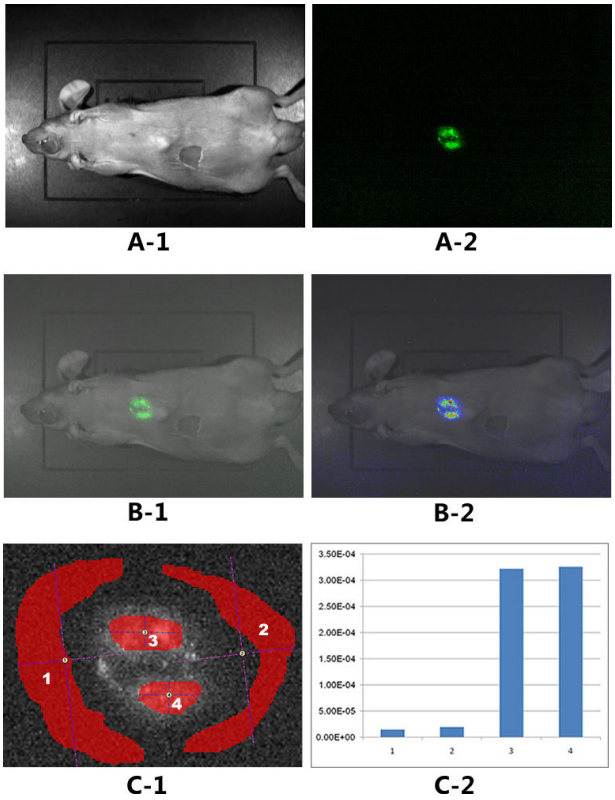

Fig .7 In vivo imaging of NaYF4: Yb, Ho nanoparticles injected into the deep tissue with the multispectral analysis. (A-1: the white image; A-2: green visible fluorescence by scanning the corresponding waveband of emission light; B-1: the composite image formed from the upconversion image and the white light image; B-2: the composite image formed from the intensity distribution image and the white light image; C-1: labeling the fluorescence regions and the environmental area without luminescence; C-2: S/N value)

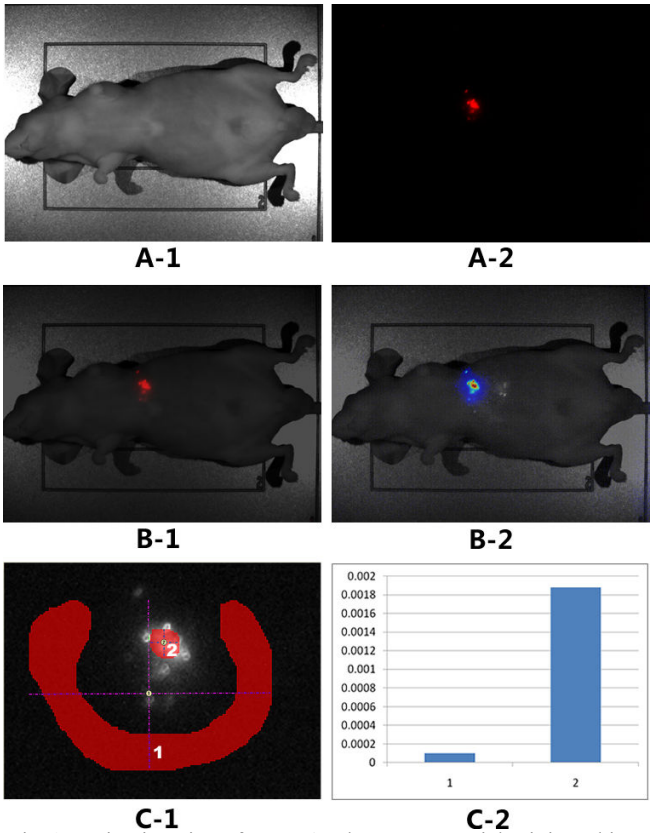

Fig .8 In vivo imaging of NaYF4: Yb, Er nanoparticles injected into the deep tissue with the multispectral analysis. (A-1: the white image; A-2: red visible fluorescence by scanning the corresponding waveband of emission light; B-1: the composite image formed from the upconversion image and the white light image; B-2: the composite image formed from the intensity distribution image and the white light image; C-1: labeling the fluorescence regions and the environmental area without luminescence; C-2: S/N value)

IV. Conclusion

UCPs emit detectable photons of higher energy in the near-infrared (NIR) or visible range upon irradiation with an NIR light in a process termed 'upconversion.' Because tissue does not perform upconversion, imaging of UCPs does not have the high background signals caused by endogenous fluorophores in fluorescence imaging. In this work, we have developed a novel instrumentation named NIR-reflected multispectral imaging system for upconversion fluorescent imaging in small animals. Based on this system, we have obtained the high contrast images without the autofluorescence when biocompatible UCPs were injected near the body surface or deeply into the tissue. Furthermore, we can extract respective spectra of the upconversion fluorescence and relatively quantify the fluorescence intensity with the multispectral analysis. This study has provided a foundation for the development of the advanced molecular imaging in small animal based on the UCPs as biological luminescent labels.

Acknowledgment

This work was supported by the National Natural Science Foundation of China (Grant No.30900346-C100602).

References

[1] S.A. Hilderbrand, and R.Weissleder, " Near-infrared fluorescence: application to in vivo molecular imaging," *Curr. Opin. Chem. Biol.* , vol. 14, pp.71-79, Feb. 2010.

[2] J.H. Rao , A. Dragulescu-Andrasi, and H.Q.Yao, "Fluorescence imaging in vivo: recent advances,"*Curr .Opin. Biotechnol*., vol. 18, pp17-25, Feb. 2007.

[3] S.L. Luo, E.L. Zhang, Y.P. Su, T.M. Cheng, and C.M. Shi, " A review of NIR dyes in cancer targeting and imaging." *Biomaterials,* vol.32, pp. 7127-7138, Oct. 2011.

[4] E. Baggaley, J.A. Weinstein, and J.A. Gareth Williams, " Lighting the way to see inside the live cell with luminescent transition metal complexes ," *Coordin. Chem. Rev.*, vol. 256, pp. 1762-1785, Aug. 2012.

[5] E. Cassette, M. Helle, L. Bezdetnaya, F. Marchal, B. Dubertret, and T. Pons, " Design of new quantum dot materials for deep tissue infrared imaging ," *Adv. Drug Delivery Rev.,* in press.

[6] A.M. Smith, H.W. Duan, A.M. Mohs, and S.M. Nie, "Bioconjugated quantum dots for in vivo molecular and cellular imaging ," *Adv. Drug Delivery Rev.,* vol. 60, pp. 1226-1240, Aug.2008.

[7] K. Schenke-Layland, I. Riemann, O. Damour , U.A. Stock, and K. Konig, "Two-photon microscopesand in vivo multiphoton tomographs – powerful diagnostic tools for tissue engineering and drug delivery." *Adv. Drug Delivery Rev.*, vol. 58, pp. 878-896, Sep. 2006.

[8] J.V. Frangioni, " In vivo near-infrared fluorescence imaging ," *Curr. Opin. Chem. Biol.,* vol.7, pp. 626-634, Oct. 2003.

[9] H.S. Mader, P. Kele, S.M. Saleh, and O.S. Wolfbeis, "Upconverting luminescent nanoparticles for use in bioconjugation and bioimaging ," *Curr. Opin. Chem. Biol.*, vol.14, pp. 582-596, Oct. 2010.

[10] D.K. Chatterjee , A.J.Rufaihah, and Y.Zhang, " Upconversion fluorescence imaging of cells and small animals using lanthanide doped nanocrystals," *Biomaterials,* vol. 29, pp.937-943, Mar. 2008.

[11] A.J. Rufaihah, and Y. Zhang, " Biocompatibility of silica coated NaYF4 upconversion fluorescent nanocrystals," *Biomaterials*, vol.29, pp. 4122-4128, Oct.2008.

[12] M. Wang, G.Abbineni, A. Clevenger, C. Mao, and S. Xu, "Upconversion nanoparticles: synthesis, surface modification and biological applications ," *Nanomedicine: N.B.M.*, vol.7, pp.710-729, Dec. 2011.